

6.4: Durable High Performance Single Layer Anti-Reflective Coatings via Wet UV Curing Technology

Jens Thies, Edwin Currie and Guido Meijers

DSM Research, PO Box 18, 6160 MD Geleen, The Netherlands

John Southwell and Chander Chawla

DSM Desotech, 1122 St Charles Street, Elgin, IL 60120, USA

Abstract

We report a novel manner for preparing single layer anti-reflective coatings with excellent optical properties (<1% reflection) over a broad wavelength regime. The technology is based upon the self-assembly and UV curing of reactive nanoparticles, leading to nano-structured coatings with a gradient in refractive index. The single processing step leading to such coatings is fast, robust and cost effective. Furthermore in this paper we will address the mechanical durability of such nano-structured coatings.

1. Objective and Background

Surface reflections are problematic in various display applications, as they greatly reduce the contrast and legibility of the displayed image. Hence anti-reflective (AR) coatings are used in a wide variety of information displays. Most current AR coatings rely upon destructive interference for their optical performance. However, in the case of a single inorganic coating (c.g. MgF_2) deposited upon a substrate such as glass or PET, the AR performance is limited to a narrow wavelength regime, and the residual reflectance is considerable. High performance AR coatings (i.e. <1% reflection) are often multi-layer systems (4-6 inorganic layers), where the layer thickness and refractive index of each layer is precisely controlled to produce anti-reflective coatings system with broad-band optical performance.¹⁻³

Multi-layered systems are predominantly prepared by vapour deposition techniques and are therefore time-consuming, laborious and as a result expensive.⁴⁻⁵ Thermal or UV curable coatings that are processable via wet deposition techniques are faster and more cost effective, but have not achieved the same balance of optical performance and durability of vapour deposited AR coating systems thus far.

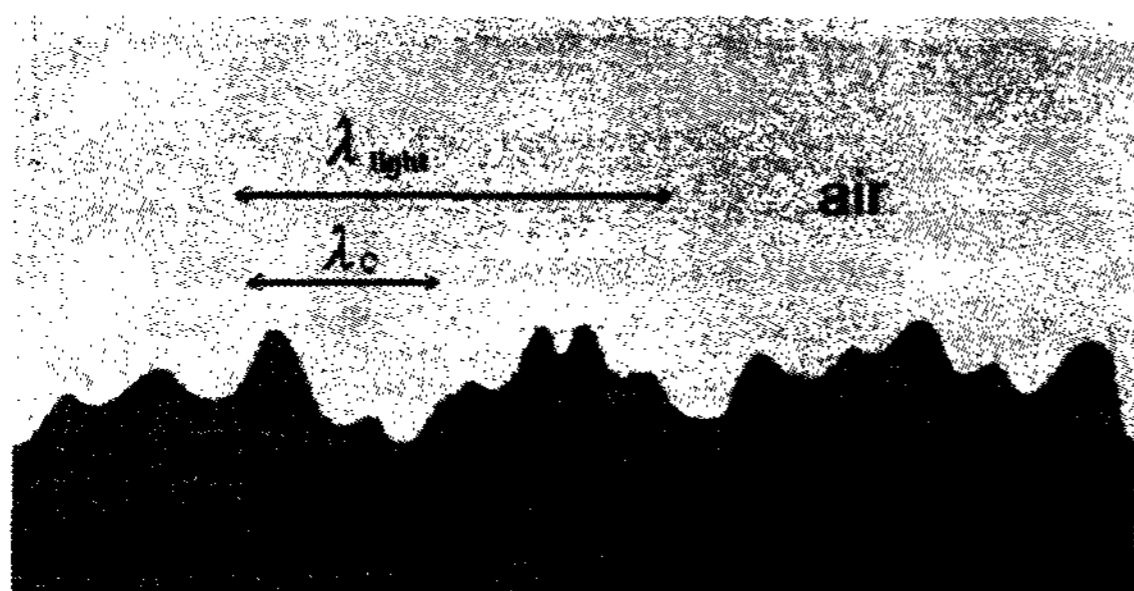


Figure 1. Schematic representation of a nano-structured surface capable of anti-reflective properties.

Recently there has been much interest in the use of nano-structuring of surfaces to achieve high performance AR coatings. In nano-structured AR coatings the surface of the coating possesses a degree of roughness, as shown schematically in Figure 1. The requirements for this roughness or surface topography are twofold. First, the average distance between features on the surface (λ_c) should be less than the shortest wavelengths of visible light (<400 nm). This will ensure that the surface topography does not scatter incident light, leading to coatings which appear colored or opaque.³ Second,⁶ the features should have an average height between 50 and 150 nm. The consequence of this is that incident light experiences a gradient of increasing refractive index as it passes from air into the bulk of the coating (we return to this in the section on optical modeling). In this sense, the modus operandi of a nano-structured AR coating differs from that of conventional single or multilayer AR coatings, which predominantly rely upon destructive interference.

Nano-structured AR coatings have to date been prepared via two approaches: a) direct reproduction of corrugation features (c.g. the Fraunhofer technique via lithography and embossing)⁷ or b) via phase-separation techniques. Although direct reproduction allows total control over the size and height of the features, it has several drawbacks, not the least being that the process is not scale-independent. This entails that the effort to produce a coated surface is roughly proportional to the size of the surface. Spontaneous processes are scale-independent, i.e. the effort to produce a cm^2 or m^2 coated area is roughly the same. Reported phase separation approaches involve the removal of one of the phase-separated components by a washing step; the phase separation can be induced thermally upon evaporation of a solvent⁸ or by photo-crosslinking.⁹

Although an elegant solution, these phase separation techniques suffer from inherent problems. Most importantly, as phase separation is a dynamic process, the size of the features and hence the optical properties are predominantly determined by phase separation kinetics. Hence optical reproducibility may be problematic when there is, for example, a change in temperature. Moreover, in the case of photo-induced phase separation the intensity of the radiation used, the amount of photo-initiator and the quantum efficiency all contribute to the final topography. Furthermore the need for removal of one of the phase-separated components by washing with solvent also introduces an additional, undesirable processing step.

In our opinion there is a need for high performance single layer AR coatings with a nano-structured surface that is formed spontaneously upon evaporation of the application solvent and where the surface topography, and thus the optical performance, are independent of the curing conditions.¹⁰ In this paper we present such coatings and discuss their preparation and properties.

2. Method

Single layer AR coatings were prepared by self-assembly and subsequent crosslinking of reactive nano-particles. Reactivity is introduced through surface modification of the nano-particles with reactive groups capable of forming a polymeric network, for example acrylate groups. The reactive nano-particles were applied to a substrate from suspension, in the presence of reactive diluents, using an organic solvent, for example isopropyl alcohol (IPA) or methyl ethyl ketone (MEK). All conventional deposition techniques are suitable for this process, e.g. dip-coating, spin-coating or roll-to-roll processing. Subsequently the solvent was evaporated prior to crosslinking, which was achieved thermally and/or photo-chemically. The thickness of the resultant coatings was between 100 and 200 nm, depending on the desired optical properties. The coatings were prepared either on Si-wafers (AFM images) or standard PET films of 125 μm thickness.

The optical properties (reflection) of the coated substrates were measured using a Minolta CM-3700d spectrophotometer. The thickness of the coating was determined on Si-wafers using a F20 multi-spectral reflectometer from AG Electro Optics.

Atomic Force Microscopy images of the prepared coatings were made using a Digital Instruments AFM in the tapping mode and Abbott curves were generated using SPIP (Scanning Probe Image Processor) Version 3.001 software from Image Metrology.

3. Surface Topology

Following the method outlined above leads to coatings with nano-structured surface topographies, an example of which can be seen in the AFM images given in Figure 2 below.

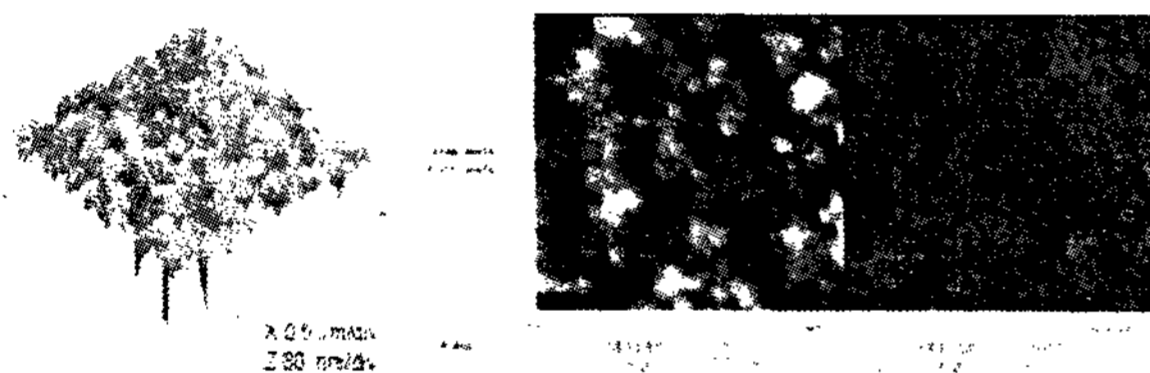


Figure 2. AFM images of a nano-structured AR coating formed (after UV curing) by self-assembly of reactive nano-particles.

The images depicted in Figure 2 show a typical example of the topography of the prepared AR coatings. The left image depicts a 3D representation of the sample, where the sample area is $2 \times 2 \mu\text{m}$ and the z-axis, depicting the height difference, is 140 nm. The middle image shows the topology from above in terms of height difference. The right image is the phase imaging of the topology, which demonstrates that the coating composition is homogeneous from the point of view of viscoelastic properties.

In Figure 3 cross-sectional AFM images of the same coating are shown. As discussed previously in the Introduction, both the height and lateral distance of the features should be within certain critical limits and from Figure 3 it is clear that our coatings are well within these boundaries.

Another way of depicting the topology, which gives direct insight into the density gradient of the surface, is by generation of an

Abbott-curve. In this case an AFM-image is integrated laterally over the total image area, resulting in a curve that shows the percentage of coverage as a function of the depth. In Figure 4 such an image is shown, and it is clear that the density gradient, which corresponds directly with a refractive index gradient, has a spatial extent of roughly 60 nm.

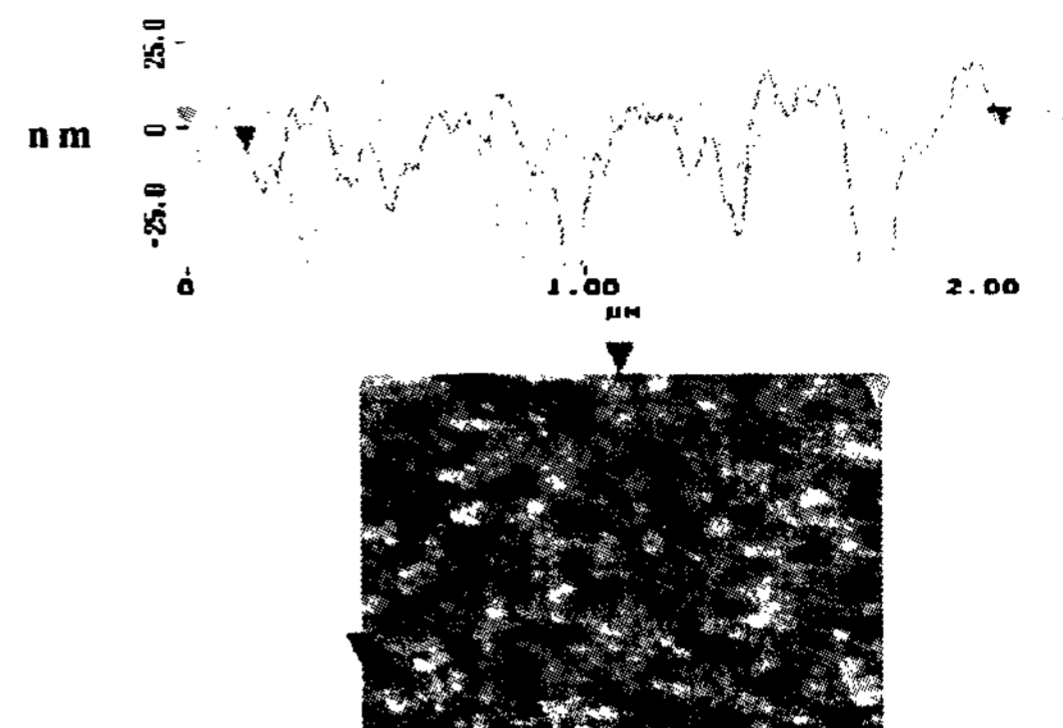


Figure 3. Cross-sectional AFM image of nano-structured AR coatings formed (after UV curing) by self-assembly of reactive nano-particles (y axis in nm, x axis is μm).

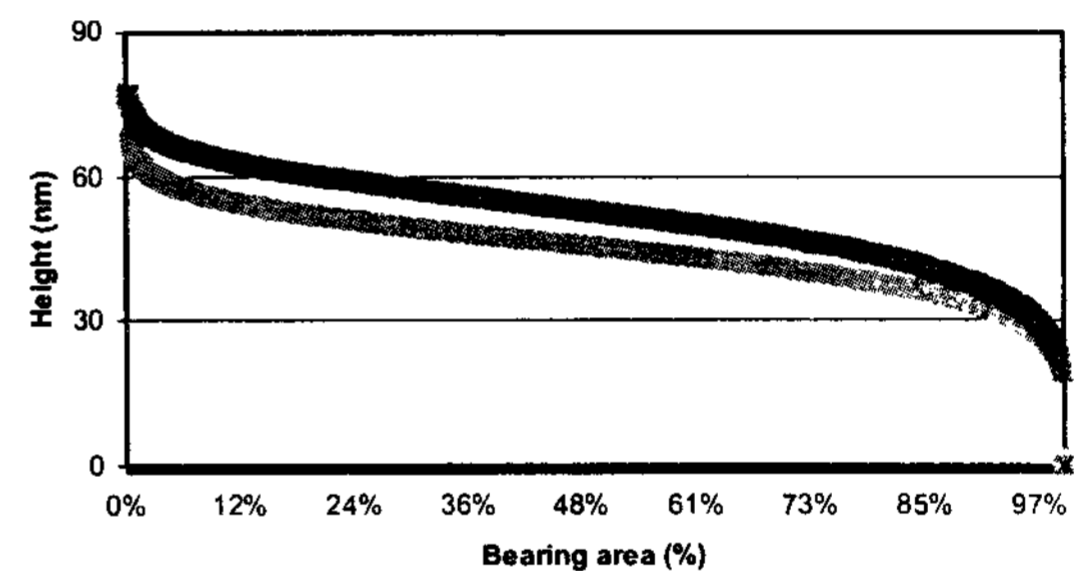


Figure 4. Abbott curves of two nano-structured coatings.

4. Optical Properties

The effect of the topography of the nano-structured AR coating on the reflectivity of a standard PET film is demonstrated in Figure 5. Applying the AR coating to both sides of a PET film by dip coating reduced the inherent reflection of the PET from $10.7 \pm 0.1\%$ at 550 nm to $0.7 \pm 0.1\%$ at the same wavelength. The reflectivity of the AR-coated PET had a minimum around 500 nm.

The wavelength at which this minimum occurs is controlled via the processing conditions (coating thickness). By varying the conditions the minimum can be shifted between 400 and 700 nm. At the same time the transmission of our coatings is above 98% with the maximum occurring at the wavelength where the minimum in reflection was observed (not shown). The decrease in

(specular) reflection is therefore not due to non-specular scattering, but is accompanied with a substantial increase in transmission, as was expected for non-scattering AR coatings.

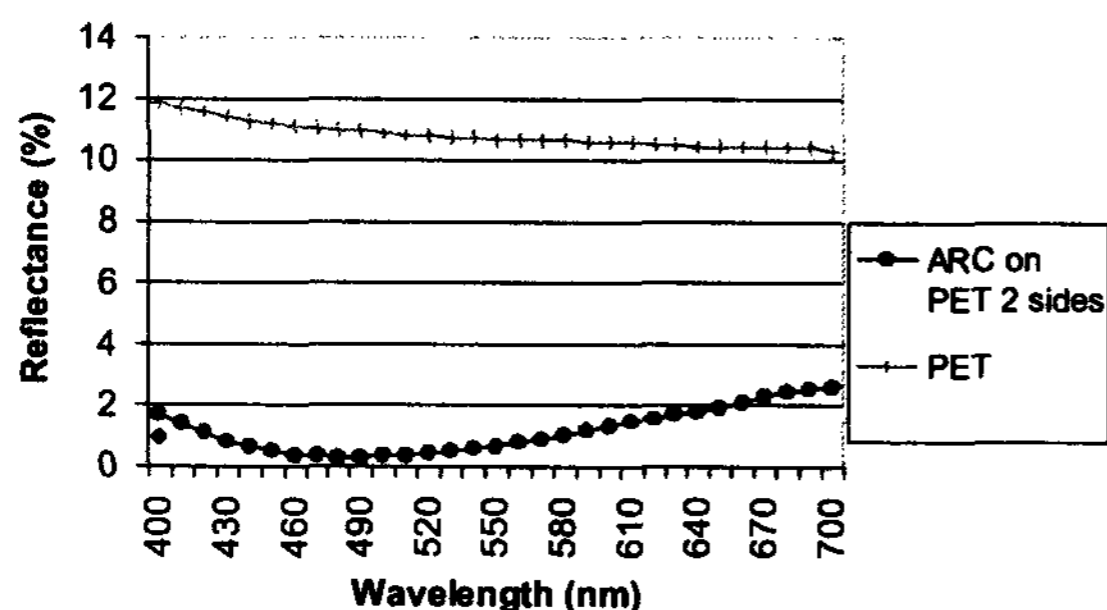


Figure 5. Reflectivity spectra of untreated PET film and a similar PET film coated on both sides with a nano-structured AR coating.

5. Mechanical Durability

The anti-reflective coatings we have developed come with range optical and mechanical properties. In order to achieve this the anti-reflective coating is applied on top of specially developed hard coats. In general terms the reflectivity of durable systems with a pencil hardness¹¹ of ca 2H-3H is in the region of 1% at 550nm, see figure 7. The surface after pencil hardness testing was observed by scanning electron microscopy (SEM) and the resultant images can be seen in figure 6.

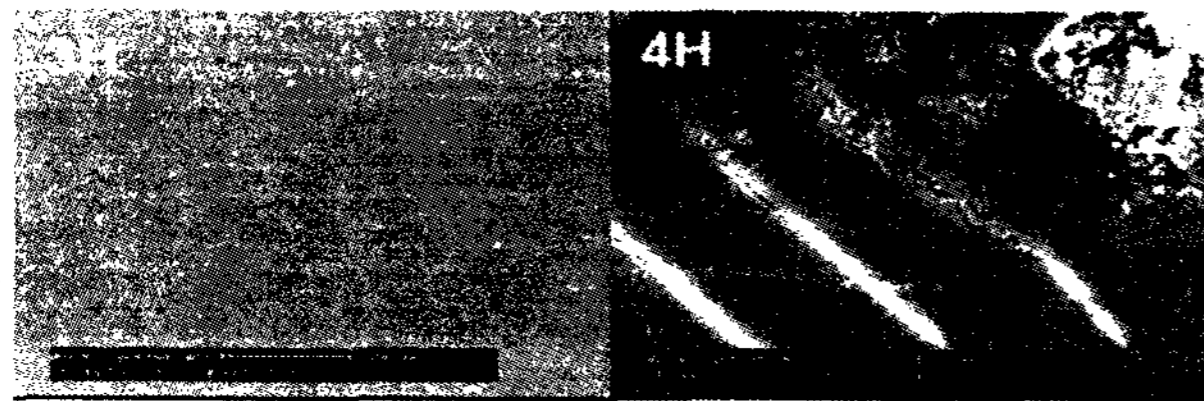


Figure 6. SEM images of AR coating surface on hard coat after pencil hardness testing with 3H and 4H pencil.

The SEM image in figure 6 shows that, while there is a deposition of graphite from the pencil in the case of the 3H test, catastrophic coating failure only occurs at 4H for this system.

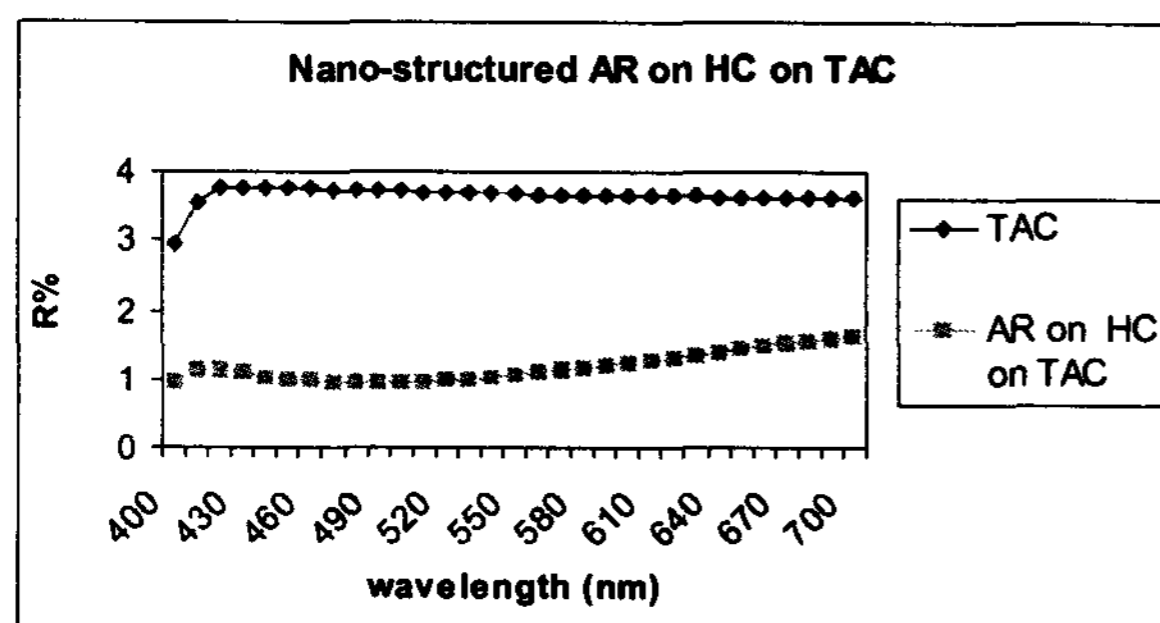


Figure 7. Reflectivity spectra of one side of an untreated TAC film and a TAC film coated on one side with AR and hard coating.

Furthermore nano-indentation has been used to study the mechanical properties of such thin nano-structured coatings. The technique and results will be discussed in more detail in this paper.

6. Impact

It is our belief that the technology outlined in this paper can have far reaching impact in the display area. Our AR technology presents a combination of fast and reproducible processing with excellent optical properties, which will allow for the application of such coatings on flexible substrates for many types of displays using, for example, roll-to-roll application. Furthermore the technology is applicable to other substrates such as glass and optionally curved substrates, which are inherently difficult to coat using vapour deposition techniques. The use of UV photopolymerisation is advantageous in that the curing process is extremely fast. The AR performance is independent of the UV curing kinetics and hence a change of UV light intensity, photo-initiator levels and/or temperature have very little or no effect on the optical properties.

The topography and bulk morphology of the nano-structured AR coating, and hence its optical properties, can be altered by controlling the parameters of the self-assembly process. Also, for mechanical robustness deposition of the AR coating on a hard-coat is possible, which is shown to have little effect on the overall optical properties.

7. Acknowledgements

We would like to thank Renate Tandler of DSM-Research for the AFM images and Dr. K. Bastiaansen of the Technical University Eindhoven for help with optical measurements.

8. References

- [1] R.J. Hill and S.J. Russel, "Coated Glass application and markets", BOC Coating Technology, ISBN no 0-914289-01-2 (1999).
- [2] D. Chen, Solar Energy Materials and Solar Cells, 68, p. 313-336 (2001).
- [3] H.J. Gläser, Large Area Glass Coating, Von Ardene, ISBN no 3-00-004953-3 (2000).
- [4] K. Abate, The Chemist, May-June, p. 9 (2001).
- [5] R.J. Hill and R.E. Keough, International Glass Review, Issue 3, p. 52-56 (1999).
- [6] S.F. Munro, J. of Opt. Soc. Am., 51 p. 280-282 (1961).
- [7] V. Boerner *et al*, SID Conference Proceeding, 7.3, p. 68-71 (2003).
- [8] U. Steiner *et al*, Science, vol 283, p. 520 (1999).
- [9] M. Ibn-Elhaj and M. Schadt, Nature, vol 410, p. 796 (2001).
- [10] Bautista & Morales, Solar Energy Materials & Solar Cells, vol 80, p. 217-225 (2003).
- [11] ASTM International, Designation D3363-00